Inorganic Chemistry

Article

pubs.acs.org/IC

Diruthenium(III,III) Bis(alkynyl) Compounds with Donor/Acceptor-Substituted *geminal*-Diethynylethene Ligands

William P. Forrest, Zhi Cao, Kerry M. Hassell, Boone M. Prentice, Phillip E. Fanwick, and Tong Ren*

Department of Chemistry, Purdue University, West Lafayette, Indiana 47907, United States

Supporting Information

ABSTRACT: Reported in this contribution are the preparation and characterization of a series of $Ru_2(DMBA)_4$ (DMBA = *N*,*N*′-dimethylbenzamidinate) bis(alkynyl) compounds, *trans*-$Ru_2(DMBA)_4$(X-*gem*-DEE)$_2$ [*gem*-DEE = *σ*-*geminal*-diethynylethene; X = H (**1**), Si^iPr_3 (**2**), Fc (**3**); 4-$C_6H_4NO_2$ (**4**), and 4-$C_6H_4NMe_2$ (**5**)]. Compounds **1**−**5** were characterized by spectroscopic and voltammetric techniques as well as the single-crystal X-ray diffraction studies of **2** and **3**. Both the single-crystal structural data of compounds **2** and **3** and the spectroscopic/voltammetric data indicate that the *gem*-DEE ligands are similar to simple acetylides in their impact on the molecular and electronic structures of the $Ru_2(DMBA)_4$ core. Furthermore, density functional theory calculations revealed more extensive *π* delocalization in aryl-donor-substituted *gem*-DEEs and that the hole-transfer mechanism will likely dominate the charge delocalization in Ru_2-*gem*-DEE-based wires.

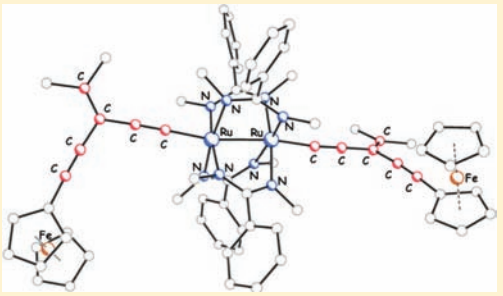

INTRODUCTION

During the past several decades, a great deal of research has been directed toward the design and synthesis of conjugated organic compounds having extensive *π* delocalization and highly polarizable *π*-electron systems. These compounds continue to be sought-after materials because of their interesting optical and conductive properties as well as their nonlinear optical responses (NLOs) or large molecular first- and second-order hyperpolarizabilities (*β* and *γ*, respectively).[1] By far, linearly conjugated *π*-electron systems [Chart 1; polyacetylene (**I**), polydiacetylene (**II**), and polytriacetylene (**III**)] are the most researched and well-known. In addition, several other types of conjugation also display interesting electronic features, i.e., *σ* conjugation in polysilanes,[2] *σ*−*π* conjugation in oligo(cyclohexylidene),[3] and homoconjugation in diphenylpropanes and diphenylsilianes.[4] A type of conjugation that is of significant interest to physical organic chemists but far is less investigated is *cross-conjugation*, which is defined as the conjugation of two unsaturated moieties to a third unsaturated fragment without being directly conjugated to each other.[5] The most apparent difference between linearly conjugated and *cross-conjugated* organic molecules is that the *π*-electron density is not as easily delocalized along the carbon framework within *cross-conjugated* molecules, which is in concurrence with classical resonance theory.[5] The rapid progress in the synthesis of nonlinear eneyne and enediyne scaffolds, notably the contributions from Nielsen and Diederich,[6] Tykwinski and co-workers,[7] and Hopf,[8] make it possible to explore *cross-conjugated* organic and organometallic compounds based on scaffolds of mixed acetylene and ethene units.

Chart 1. *π*-Conjugated Eneyne and Enediyne Oligomers

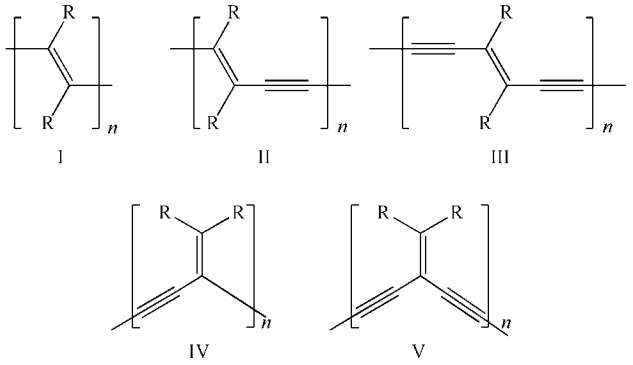

Cross-conjugated oligomers based on the eneyne framework, such as isopolydiacetylenes (Chart 1, **IV**)[9,10] and isopolytriacetylenes (Chart 1, **V**),[11,12] have been previously studied and have shown that electronic communication is observed along the eneyne framework.[13] Organic compounds containing the *geminal*-diethynylethene unit (or isotriacetylene, abbreviated as *gem*-DEE) are of particular interest because it has been recently suggested on the basis of computational modeling that oligomers of *gem*-DEE may function as molecular wires with conductance attenuated by quantum interference effects.[14] We hypothesize that the combination of a redox-rich transition metal with donor/acceptor-substituted *gem*-DEE frameworks will provide a set of organometallic compounds for the experimental exploration of *cross-conjugation* and quantum interference effects.

Received: December 19, 2011
Published: February 10, 2012

   dx.doi.org/10.1021/ic202720c | *Inorg. Chem.* 2012, 51, 3261−3269

Transition-metal compounds containing linear arylacetylide and polyynyl ligands have been studied for several decades with efforts focusing on the linear π conjugation therein,[15,16] and efficient charge transfer has been documented for polyynyl/polyenyl compounds of metal centers such as iron,[17] rhenium,[18] and ruthenium.[19] However, transition-metal compounds with nonlinear eneynes or enediynes as σ-acetylide ligands are relatively rare, and ones based on *gem*-DEE are strictly limited to platinum(II) species.[20] It is worth noting that the coordination of tetraethynylethene, a ligand related to *gem*-DEE, to metal centers such as platinum(II),[21] gold(I),[22] and iron(II)[23] and a trimetallic cluster $(\mu_3\text{-C})Co_3$[24] have been documented as well. While the platinum(II) examples demonstrate the feasibility of metalation, the π conjugation between *gem*-DEE and the platinum(II) center is limited because of the electronic saturation of a d^8 configuration in a square-planar environment. Hence, there is the need to prepare *gem*-DEE complexes of redox-active transition metals, which will help to elucidate the effect of *cross-conjugation* in metal-*gem*-DEE systems. Previously, we communicated the syntheses of two *trans*-$Ru_2(DMBA)_4$(X-*gem*-DEE)$_2$ compounds [X = H (**1**) and Si^iPr_3 (**2**), DMBA = *N*,*N*′-dimethylbenzamidinate, and *gem*-DEE = σ-*geminal*-diethynylethene], which were the first examples of redox-active transition-metal complexes containing *gem*-DEE ligands.[25] In this contribution, we expand the investigation of $Ru_2(DMBA)_4$(X-*gem*-DEE)$_2$-type complexes to those containing electron-donor, ferrocenyl (Fc) and 4-(dimethylamino)phenyl (DMAP), or electron-acceptor, 4-nitrophenyl (NP), substituted *gem*-DEEs as the axial σ-acetylide ligands (Scheme 1).

Scheme 1. $Ru_2(DMBA)_4$ Compounds of *gem*-DEE Ligands

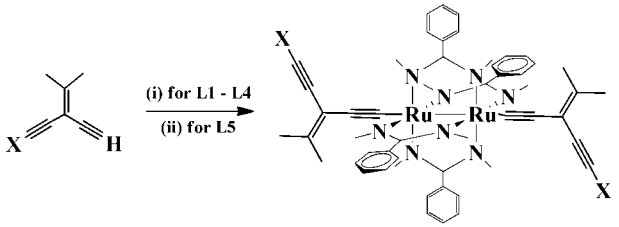

RESULTS AND DISCUSSION

Synthesis. The X-*gem*-DEE ligands **L1**−**L5**, as shown in Scheme 1, were prepared according to the literature methods. The initial synthesis of metal compounds started with 1-(trimethylsilyl)-3-(trimethylsilyl)ethynyl-4-methylpent-3-en-1-yne,[10] which was converted to 3-ethynyl-4-methylpent-3-en-1-yne (**L1**) upon desilylation using K_2CO_3. Ligands **L2** and **L3** were desilylated using methanolic K_2CO_3, while ligands **L4** and **L5** were desilylated using aqueous *n*-Bu_4NF. Ligands **L1**, **L2**, and **L5** were isolated as clear oils, while ligands **L3** and **L4** were isolated as orange and yellow solids, respectively.

The *trans*-$Ru_2(DMBA)_4$(X-*gem*-DEE)$_2$-type compounds were prepared using the weak-base-assisted reaction.[26,27] The reaction between $Ru_2(DMBA)_4(NO_3)_2$[26] and **L1** in the presence of Et_3N readily yielded a red solution that is characteristic of $Ru_2(DMBA)_4(C_2R)_2$-type compounds.[27] Thin-layer chromatography (TLC) analysis of the reaction mixture after 3 h, however, revealed that, in addition to a red species [R_f = 0.72, 1:3 (v/v) EtOAc/hexanes], there was a long, reddish-brown band not far from the baseline. The red species was isolated via recrystallization in 20% yield and unambiguously identified as *trans*-$Ru_2(DMBA)_4$(H-*gem*-DEE)$_2$ (**1**) through both ^{1}H NMR and high-resolution nano-electrospray ionization mass spectrometry (HR-nESI-MS). We surmised that the appearance of very polar byproducts in the synthesis of **1** is likely due to the formation of oligomerized species attributed to the presence of the free ethynyl (−C≡CH) in **1**, which may displace a coordinated **L1** to yield a dimer bridged by μ-C,C′-*gem*-DEE, and subsequently trimer, etc. To eliminate the possibility of oligomerization, our attention turned to 1-(triisopropylsilyl)-3-(trimethylsilyl)ethynyl-4-methylpent-3-en-1-yne,[10] which retains the triisopropylsilyl (TIPS) group to yield 1-(triisopropylsilyl)-3-ethynyl-4-methylpent-3-en-1-yne (**L2**) upon treatment with methanolic K_2CO_3. The ensuing reaction between $Ru_2(DMBA)_4(NO_3)_2$ and **L2** under weak base conditions yielded a red compound as the sole product (isolated yield 77%) after 3 h, while no residual $Ru_2(DMBA)_4(NO_3)_2$ was detected. The red product was unambiguously identified as *trans*-$Ru_2(DMBA)_4$(^{i}Pr$_3$Si-*gem*-DEE)$_2$ (**2**) through ^{1}H NMR, HR-nESI-MS, and a single-crystal X-ray diffraction study.

A similar reaction between $Ru_2(DMBA)_4(NO_3)_2$ and H-*gem*-DEE-Fc (**L3**) progressed slower than those with **L1** and **L2**: while the formation of $Ru_2(DMBA)_4$(Fc-*gem*-DEE)$_2$ (**3**) was significant, residual $Ru_2(DMBA)_4(NO_3)_2$ remained present after 3 h. The desired compound **3** was isolated via recrystallization from tetrahydrofuran (THF)/hexanes in 48% yield and was positively identified through ^{1}H NMR, HR-nESI-MS, and a single-crystal X-ray diffraction study. On the other hand, the reaction between $Ru_2(DMBA)_4(NO_3)_2$ (1 equiv) and H-*gem*-DEE-NP (**L4**; 2.2 equiv) proceeded to completion in 3 h, and *trans*-$Ru_2(DMBA)_4$(NP-*gem*-DEE)$_2$ (**4**) was isolated in 68% yield after recrystallization from THF/hexanes.

The preparation of *trans*-$Ru_2(DMBA)_4$(DMAP-*gem*-DEE)$_2$ (**5**), a strong donor-substituted compound, proved to be challenging. When H-*gem*-DEE-DMAP (**L5**; 2.2 equiv) and $Ru_2(DMBA)_4(NO_3)_2$ (1 equiv) reacted in the presence of Et_2NH in THF, substantial quantities of starting materials remained after 5 h. The desired product **5** was isolated via recrystallization from THF/hexanes in 27% yield and was positively identified through ^{1}H NMR and HR-nESI-MS. Alternatively, the Me_3Si-protected DMAP ligand (Me_3Si-*gem*-DEE-DMAP) and 1 equiv of $Ru_2(DMBA)_4(NO_3)_2$ were reacted in the presence of excess K_2CO_3 in THF/MeOH (2:1, v/v), where K_2CO_3 was used for both desilylation and as a base for metalation. Compound **5** was obtained in a similar yield after reaction overnight. Finally, a high-yield preparation of **5** was achieved from the reaction between $Ru_2(DMBA)_4Cl_2$ and 2.2 equiv of Li-*gem*-DEE-DMAP (Li-**L5**), a method that was successful in affording $Ru_2(DMBA)_4(C{\equiv}CC_6H_4\text{-}4\text{-}NMe_2)_2$ in high yield.[28] The reaction between Li-**L5** and $Ru_2(DMBA)_4Cl_2$ was almost instantaneous based on the color change, and subsequent recrystallization of the reaction mixture from EtOAc/hexanes resulted in **5** in high yield (74%).

Molecular Structures of 2 and 3. Further confirmation of the identity of *trans*-$Ru_2(DMBA)_4$(X-*gem*-DEE)$_2$-type compounds came from the single-crystal X-ray diffraction study of **2** and **3**.

dx.doi.org/10.1021/ic202720c | *Inorg. Chem.* 2012, 51, 3261−3269

The molecular structures determined for **2** and **3** are shown in Figures 1 and 2, respectively, and the selected bond lengths and

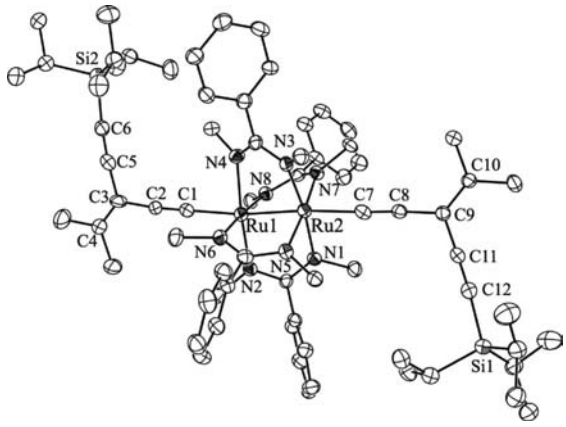

Figure 1. ORTEP plot of **2** at 20% probability. H atoms were omitted for clarity.

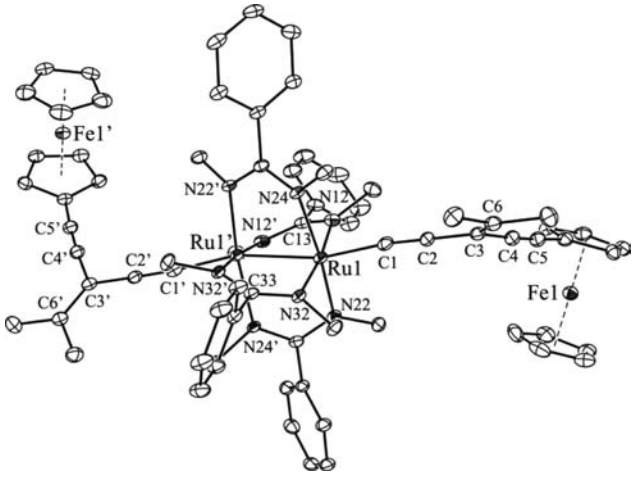

Figure 2. ORTEP plot of **3** at 20% probability. H atoms were omitted for clarity.

angles are listed in Table 1. While the asymmetric unit of crystal **2** contains a complete Ru_2 molecule, the asymmetric unit of **3** contains only half of the Ru_2 molecule, which is related to the other half through a crystallographic 2-fold axis defined by the C13 and C33 atoms. The geometric parameters around the first coordination sphere of the Ru_2 core are comparable to those of other $Ru_2(DMBA)_4(C{\equiv}CR)_2$-type compounds.[29] The Ru−Ru bond lengths are 2.4624(9) and 2.4569(4) Å for **2** and **3**, respectively, while those of $Ru_2(DMBA)_4(C{\equiv}CR)_2$ are in the range of 2.441−2.476 Å. The Ru−C bond distances in **2** and **3** are 1.981 and 1.974 Å, respectively, which are in agreement with those determined for other $Ru_2(DMBA)_4(C{\equiv}CR)_2$ compounds (1.95−2.00 Å). These data indicate that the *gem*-DEE ligand behaves similarly to simple acetylides in bonding to the Ru_2 core. Typical of diruthenium(III,III) compounds bearing strong axial donor ligands, the arrangement of the equatorial N-donor atoms deviates significantly from the eclipsed D_{4h} symmetry.[30] The eight N atoms fall into two distinct groups, those of elongated Ru−N bonds and those of shortened Ru′−N′ bonds, which also span a large torsional angle N−Ru−Ru′−N′ (avg. 19.2°). The electronic origin of such structural distortion has been attributed to both a second-order Jahn−Teller effect and the formation of a partial σ(Ru−Ru)

Table 1. Selected Bond Lengths (Å) and Angles (deg) for Compounds 2 and 3

2		**3**	
Ru1−Ru2	2.4624(9)	Ru1−Ru1′	2.4569(4)
Ru1−C1	1.982(9)	Ru1−C1	1.974(4)
Ru2−C7	1.979(9)		
Ru1−N2	2.105(6)	Ru1−N12	2.025(2)
Ru2−N1	2.004(7)	Ru1−N22	2.043(2)
Ru1−N4	1.973(6)	Ru1−N32	1.991(2)
Ru2−N3	2.074(6)	Ru1−N24	2.133(2)
Ru1−N6	2.001(6)		
Ru2−N5	2.127(6)		
Ru1−N8	2.101(6)		
Ru2−N7	1.977(6)		
C1−C2	1.198(11)	C1−C2	1.224(5)
C3−C4	1.321(14)	C3−C6	1.353(5)
C5−C6	1.209(12)	C4−C5	1.188(5)
C7−C8	1.215(11)		
C9−C10	1.343(10)		
C11−C12	1.190(11)		
Ru1−C1−C2	176.1(8)	Ru1−C1−C2	174.0(3)
Ru2−C7−C8	176.6(8)		
C2−C3−C5	110.5(8)	C2−C3−C4	124.0(3)
C8−C9−C11	113.2(7)		
C1−Ru1−N6	96.8(3)	C1−Ru1−N32′	100.3(12)
C1−Ru1−N8	89.0(3)	C1−Ru1−N12′	86.40(11)
C1−Ru1−Ru2	165.3(3)	C1−Ru1−Ru1′	164.64(9)
N2−Ru1−Ru2−N1	19.55(0.26)	N24′−Ru1′−Ru1−N22	20.80[a]
N4−Ru1−Ru2−N3	18.15(0.27)	N22′−Ru1′−Ru1−N24	17.68[a]
N6−Ru1−Ru2−N5	19.47(0.26)		
N8−Ru1−Ru2−N7	19.67(0.26)		

[a]Determined in *PLUTON*.

bond based on dπ-type orbitals[30,31] and will be elaborated in the density functional theory (DFT) calculation section.

While both TIPS-*gem*-DEE ligands are approximately coplanar with the framework defined by the N1−N2−N4−N3 linkage in **2**, only one of the Fc-*gem*-DEE ligands in **3** is coplanar and the second is perpendicular to the N22−N24′−N24−N22′ framework. In compound **2**, the two (triisopropylsilyl)ethynyl fragments are oriented in the opposite directions. In compound **3**, the two Fc's are approximately in an orthogonal orientation.

The bond lengths and angles of the TIPS-*gem*-DEE ligands in **2** are in close agreement with those determined for a free *gem*-DEE ligand (TMS-*gem*-DEE-TMS).[12] Both the ruthenium-bound acetylene bond (C1−C2) and the "free" alkyne bond (C5−C6) are of length similar to those in TMS-*gem*-DEE-TMS [1.191(6) and 1.215(6) Å, respectively]. There are two notable bond angles: (1) the alkylidene angle C2−C3−C5 at 110.5(8)°, which is less than the anticipated angle of 120° for an sp^2-hybridized C atom and (2) the Ru−C≡C angle of 176°, which is slightly distorted from linearity, demonstrating the inherent flexibility that the alkynyl bonds often show in the solid state.[16] Tykwinski and co-workers reported the X-ray structures of a series of donor/acceptor-substituted *gem*-DEEs,[32] and the geometric parameters of the diethynylethene framework were quite constant regardless of the nature of the substituents.

Electrochemistry. Typically, $Ru_2(DMBA)_4(C_2R)_2$-type compounds undergo at least two diruthenium-centered one-electron couples: an oxidation (**A**) and a reduction (**B**), as can be clearly seen in the voltammograms of $Ru_2(DMBA)_4(C_2TIPS)_2$ (**6**)

dx.doi.org/10.1021/ic202720c | *Inorg. Chem.* 2012, 51, 3261−3269

in Figure 3 and the electrode potentials in Table 2. For unsubstituted *gem*-DEE compounds **1** and **2**, both couples **A**

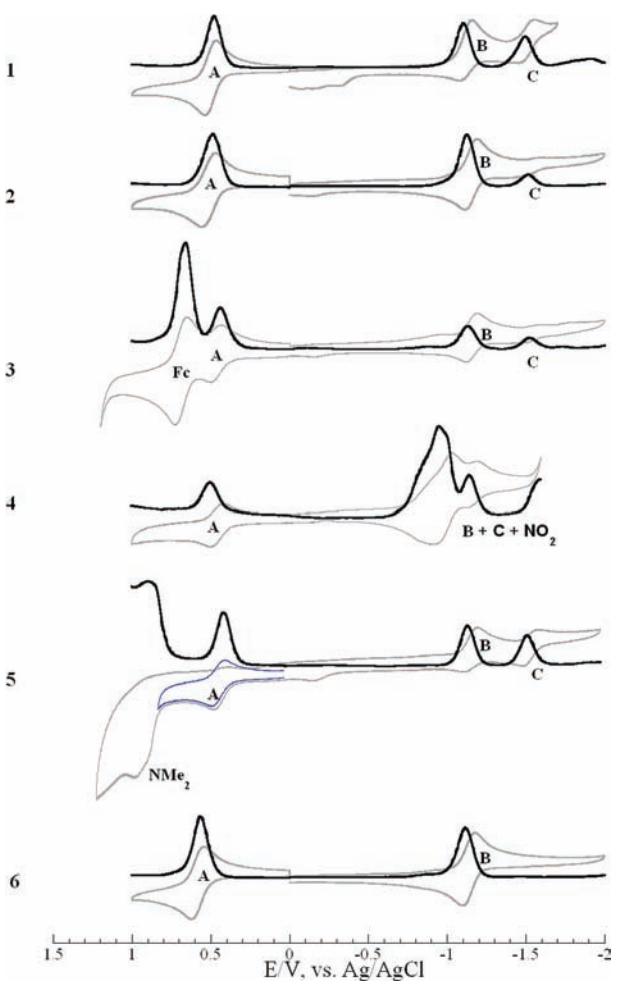

Figure 3. Cyclic (CV; gray) and differential-pulse voltammograms (DPV; black) recorded for compounds **1**–**6** in a 0.20 M THF solution of Bu_4NPF_6 at a scan rate of 0.10 V s^{-1} for CV and a pulse width of 0.05 s for DPV. The blue inset in **5** indicates the anodic CV sweep between 0 and 0.80 V.

Table 2. Electrochemical Potentials (V, vs Ag/AgCl) of Compounds 1–6

compound	*E*(**A**)	*E*(**B**)	*E*(**C**)
1	0.502	−1.154	−1.514[a]
2	0.496	−1.159	−1.496[a]
3	0.467	−1.156	−1.552[a]
4	0.485	NA	NA
5	0.448	−1.165	−1.541
6	0.585	−1.138	NA

[a]The irreversible couple, E_{pc}, is reported.

and **B** can be easily discerned from their voltammograms. The potentials of the oxidation couple (**A**) in **1** and **2** were cathodically shifted by ca. 90 mV from that of **6**, reflecting the stronger donor nature of *gem*-DEE. Unlike **6**, compounds **1** and **2** also exhibit an irreversible reduction (**C**) at ca. −1.5 V, which cannot be attributed to a second one-electron reduction of the diruthenium center in **1**/**2** because this reduction typically occurs at electrode potential < −2.0 V.[33] Instead, the partial dissociation of one of the *gem*-DEE ligands upon the first reduction resulted in a mono-*gem*-DEE-$Ru^{II,III}_2$ species, which, as a neutral species, was reduced at a mild potential (Scheme 1). Facile degradation of **1**/**2** under reducing conditions reflects a weakened Ru–C bond with the *gem*-DEE ligand compared with simple linear acetylides. The direct detection of the proposed mono-*gem*-DEE-$Ru^{II,III}_2$ species in a voltammetric experiment is challenging because it is only produced in a minute quantity at or near the electrode surface. Nevertheless, the fragile nature of the Ru–C(*gem*-DEE) bond is evident from MS experiments: the mono-*gem*-DEE-$Ru^{II,III}_2$ peak is very pronounced in the nESI spectrum of compound **2**, while the mono-TIPS-acetylide peak is negligible in the nESI spectrum of compound **6** under identical electrospray parameters (see Figure S6 in the Supporting Information).

Having two Fc-substituted *gem*-DEE ligands, compound **3** undergoes a reversible, two-electron oxidation that is ascribed to the simultaneous oxidation of both Fc units, in addition to the diruthenium-centered couples that were observed in **1** and **2**. The simultaneous oxidation of Fc in **3** is in stark contrast with the behavior of *trans*-$Ru_2(DMBA)_4(C_{2n}Fc)_2$-type compounds reported earlier by our laboratory, where pairwise oxidations of the two Fc termini were observed for compounds of n = 1–4 and were taken as evidence of long-distance electronic coupling between two Fc centers.[34,35] Clearly, the *cross-conjugated* nature of the *gem*-DEE linker severely limited the degree of electronic coupling. In comparison with compounds **1**/**2**, the couple **A** in **3** is cathodically shifted slightly, while **B** occurs at nearly identical potential. Hence, Fc's as moderate electron donors destabilized the highest occupied molecular orbital (HOMO) but had no impact on the lowest unoccupied molecular orbital (LUMO; δ^*; see the Results and Discussion section).

The behaviors of the acceptor (donor)-substituted *gem*-DEE compounds **4** (**5**) are somewhat complicated compared with those of **1**–**3**. Compound **4**, with nitrophenyl-substituted *gem*-DEE ligands, displays a reversible oxidation **A** at an electrode potential comparable to those of **1** and **2**, indicating minimal influence of an acceptor substituent on the HOMO. The cathodic region of **4** is quite complex with an early onset of multiple reduction processes (ca. −0.7 V), and significant deposition of greenish materials on the working electrode was observed upon completion of a single sweep. It is likely that the reduction of one of the nitro groups initiated some oligomerization reaction. For compound **5**, the oxidation couple (**A**) is cathodically shifted by 50 mV from that of **2**, which is consistent with DMAP-*gem*-DEE being the most electron-rich among all of the *gem*-DEE ligands. The electron richness of DMAP-*gem*-DEE also makes its C–Ru bond very prone to cleavage, as evidenced by the large current of couple **C**. In the case of *trans*-$Ru_2(DMBA)_4(C_2C_6H_4\text{-}4\text{-}NMe_2)_2$, oxidations of the two $-NMe_2$ groups were stepwise and quasi-reversible.[28] The oxidation wave of the two $-NMe_2$ groups in **5** was broad and irreversible and accompanied by degradation of **5**. The latter resulted in the disappearance of the cathodic wave of couple **A** on the backward sweep. However, when the potential sweep window was limited to +0.80 V, a perfectly reversible oxidation was recorded in CV (shown as a blue inset in Figure 3).

Vis–Near-IR (NIR) Spectroscopy. Shown in Figure 4 are the vis–NIR absorption spectra of compounds **2**, **4**, and **5**, while those of **1**, **3**, and **6** are provided as Figure S1 in the Supporting Information. The absorption spectrum of **2** features peaks at ca. 510 ($\varepsilon \sim 15\,000$ M^{-1} cm^{-1}) and 890 nm ($\varepsilon \sim 3000$ M^{-1} cm^{-1}). The low-energy transition is attributed to the dipole-allowed

dx.doi.org/10.1021/ic202720c | *Inorg. Chem.* 2012, 51, 3261–3269

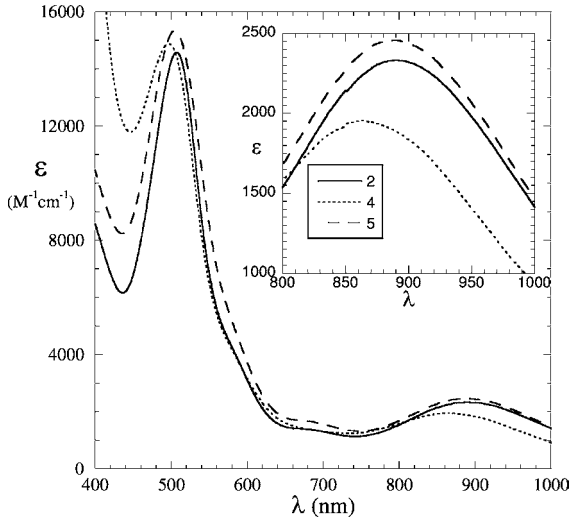

Figure 4. Vis−NIR spectra of **2** (solid), **4** (dotted), and **5** (dashed) in THF; the NIR region is magnified in the inset.

HOMO [π_{yz}*(Ru−Ru)]−LUMO [δ*(Ru−Ru)] transition, while the high-energy transition is likely due to the ligand-to-metal charge transfer from the amidinate π(N) orbital to δ*(Ru−Ru).[35] The absorption spectrum of compound **5** is very similar to that of **2** and consists of peaks at 505 nm ($\varepsilon \sim 15\,400$ M^{-1} cm^{-1}) and 890 nm (2460 M^{-1} cm^{-1}), indicating that the introduction of electron-donor aryl substituents such as DMAP do little to alter the electronic structure of **5** compared to **2**. The spectrum of **4** [497 nm (14 900 M^{-1} cm^{-1}) and 865 nm (1960 M^{-1} cm^{-1})] has both peaks blue-shifted from those of **2** and **5**.

Electronic Structures via DFT Analysis. In order to gain further insight into the electronic interactions between the donor/acceptor-substituted *gem*-DEE ligands and the Ru_2 core, DFT calculations at the B3LYP/LanL2DZ level (*Gaussian03* program)[36] were performed. In the previously reported DFT study of *trans*-$Ru_2(DMBA)_4$(*gem*-$DEE)_2$, DMBA ligands were reduced to $(HNC(H)NH)^{-1}$. In the current study, the model compound **2′** was fully optimized from the crystal structure of **2** without truncation, while the model compounds of **7**, **4′**, and **5′** were built based on the modification of **2**. Both Si^iPr_3 groups of **2** were replaced with either $-C_6H_5$ (**7**), 4-$C_6H_4NO_2$ (**4′**), or 4-$C_6H_4NMe_2$ (**5′**), which were followed by full optimizations. The optimized bond lengths and angles for **2′** are in good agreement with the crystal structural data of **2**, while comparable bond lengths and angles for the first coordination sphere of the Ru_2 core were obtained for **7**, **4′**, and **5′** (see Tables S1−S4 in the Supporting Information). The computed energies and counterplots of the most relevant molecular orbitals (MOs) for the model compounds **2′**, **7**, **4′**, and **5′** are given in Figure 5.

Compared with our prior DFT study of the simplified model compound of *trans*-$Ru_2(DMBA)_4$(*gem*-$DEE)_2$,[25] spin-restricted DFT calculations for model **2′** yielded a comparable distribution of valence MOs. The optimized Ru−Ru bond length (2.525 Å) in **2′** is longer than the experimental value of 2.462 Å in **2** but significantly shorter than that of the oversimplified model (2.611 Å) reported in the previous communication. The lengthening of the optimized Ru−Ru bond in comparison with the experimental data can be attributed to the underestimation of weak metal−metal interactions by the DFT (B3LYP) method. Similar to **2′**, the geometries optimized for **7**, **4′**, and **5′** exhibit features unique to diruthenium(III,III) bis(alkynyl) species: the nonlinearity of the −C≡C−Ru−Ru−C≡C− linkage and a distorted $Ru_2(N-N)_4$ coordination sphere (D_4 to C_2 symmetry).[30,31] The optimized Ru−Ru bond lengths for **7** (2.525 Å), **4′** (2.525 Å), and **5′** (2.521 Å) are approximately the same as that of **2′** (2.525 Å).

As shown in Figure 5, the four HOMOs of **2′**, namely, HOMO−3 to HOMO, are the combinations of $\pi(Ru_2)$ and π(*gem*-DEE). The HOMO−3 is the antibonding combination of π_{xz}(Ru−Ru) and two $\pi_{\|}$(DEE) (in-plane π orbitals of *gem*-DEE).[37] The HOMO−2 is an antibonding combination of π_{xz}*(Ru−Ru) and two $\pi_{\|}$(DEE). The π_{xz}*(Ru−Ru) component in HOMO−2 exhibits significant σ-type overlap because of the severe twisting of the equatorial DMBA ligands around the Ru_2 core, as noted in the prior study.[31] HOMO−1 and HOMO are the antibonding combinations of two $\pi_{\perp}$(DEE) (out-of-plane π orbitals of *gem*-DEE) with π_{yz}(Ru−Ru) and π_{yz}*(Ru−Ru), respectively. The LUMO is dominated by δ*(Ru−Ru) with no contribution from *gem*-DEE because of the orbital orthogonality. The LUMO+1 is mostly the contribution of two σ*(Ru−C) bonds, where the two Ru d_{z^2} orbitals have the appearance of σ-type bonding. In addition, the HOMO−4 is identified as the δ(Ru−Ru) orbital in **2′**. Furthermore, the nominal σ(Ru−Ru) is nonexistent because the d_{z^2}(Ru) orbitals are primarily used for the formation of σ(Ru−C) bonds. Hence, the ground-state configuration of the Ru_2 core is $\delta^2\pi^4\pi^{*4}$, corresponding to an effective Ru−Ru single bond.

The distribution of the valence MOs in **7** follows the same pattern as that of **2′**, albeit with a slightly enhanced HOMO−LUMO gap (1.99 in **7** vs 1.92 eV in **2′**). Compared with **2′**, both HOMO and HOMO−1 in **7** are stabilized as a result of π delocalization onto the phenyl ring, which reduces the antibonding interaction between π(DEE) and π/π*(Ru−Ru). With the introduction of a strong electron-withdrawing phenyl substituent ($-NO_2$ in **4′**), HOMO and LUMO in **4′** are further stabilized, with the HOMO−LUMO gap increasing from 1.99 eV in **7** to 2.15 eV. Both the composition and energetic order of the metal-based MOs in **4′** (with minimum contribution from nitrophenyl ligands) are almost the same as those for **7**, indicating that the electronic effect of nitro substitution is mostly inductive. In compound **5′**, the presence of a strong donating substituent ($-NMe_2$) significantly destabilized all valence MOs in comparison with those of **7** and **4′**. The electronic effect of $-NMe_2$ substitution goes beyond simply inductive: it has resulted in the substantial participation of the aryl π component in the high-lying occupied MOs. Specifically, the σ-type (in-plane) and π-type (out-of-plane) bondings of the $-C\equiv C-Ru_2-C\equiv C-$ component are apt to extensively interact with the dimethylamino-substituted phenyl rings in HOMO−2 and HOMO−1. The computed HOMO−LUMO gaps for all model compounds are in the range from 1.90 to 2.15 eV, which are comparable to that of *trans*-$Ru_2(DMBA)_4(C_2Fc)_2$.[35] Current results strongly support that the hole-transfer mechanism will likely dominate the charge delocalization in Ru_2-*gem*-DEE-based wires.

■ CONCLUSION

A new family of $Ru_2(DMBA)_4$ compounds based on substituted *gem*-DEE axial ligands were prepared under mild conditions in relatively good yields. The work described herein demonstrated the feasibility of preparing *gem*-DEE compounds of transition-metal ions beyond platinum(II). The electronic properties of

dx.doi.org/10.1021/ic202720c | *Inorg. Chem.* 2012, 51, 3261−3269

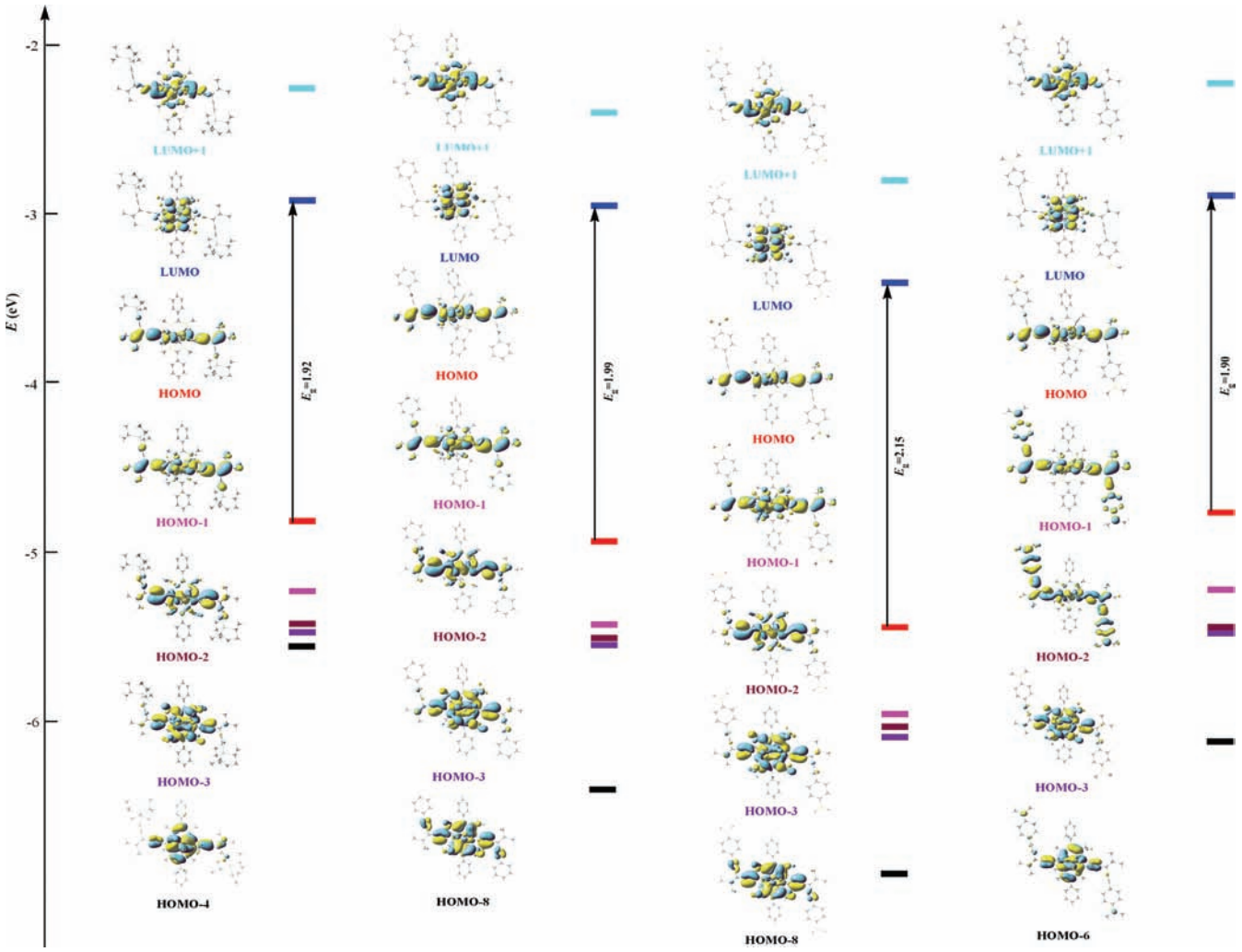

Figure 5. MO diagrams for (from left to right) **2′**, **7**, **4′**, and **5′** obtained from DFT calculations.

these new $Ru_2(DMBA)_4$ compounds having *cross-conjugated* σ-alkynyl ligands resemble those of the previously studied $Ru_2(DMBA)_4(C_2R)_2$ compounds. DFT analysis provided a better understanding of both the molecular and electronic properties for the $Ru_2(DMBA)_4$(*gem*-DEE)$_2$-type compounds. While most of the terminal substituents of *gem*-DEE manifest a minimal π interaction with the Ru_2 center, the strong donor $-NMe_2$ enables an extensive interaction between π(*gem*-DEE) and $\pi(Ru_2)$ orbitals.

EXPERIMENTAL SECTION

General Procedures. X-*gem*-DEE ligands (**L1**−**L5**) were prepared according to previously reported literature procedures.[10,38] $Ru_2(DMBA)_4(NO_3)_2$ and $Ru_2(DMBA)_4Cl_2$ were prepared as previously described.[26,33] ^{1}H NMR spectra were obtained using a Varian Mercury 300 NMR spectrometer, with chemical shifts (δ) referenced to the residual $CHCl_3$. Vis−NIR spectra were obtained with a Jasco V-670 spectrophotometer in THF solutions. Fourier transform infrared (FT-IR) spectra were measured on neat samples with a Jasco FT/IR-6300 spectrometer. nESI-MS spectra were performed on a QqQ tandem mass spectrometer in CH_2Cl_2 (QTRAP4000; Applied Biosystems/MDS Sciex, Concord, Ontario, Canada). For compounds **1**−**5**, the HR-nESI-MS spectra were performed on a modified QqTOF tandem mass spectrometer in CH_2Cl_2 (QSTAR XL; Applied Biosystems/MDS Sciex, Concord, Ontario, Canada). Masses were calculated by isotopic distribution utilizing Analyst 1.4 software (Applied Biosystems/MDS Sciex, Concord, Ontario, Canada). CV and DPV were recorded in a 0.2 M $(n\text{-Bu})_4NPF_6$ solution (THF, N_2-degassed) on a CHI620A voltammetric analyzer with a glassy carbon working electrode (diameter = 2 mm), a platinum wire auxiliary electrode, and a Ag/AgCl reference electrode. The concentration of Ru_2 species is always 1.0 mM. The ferrocenium/ferrocene couple was observed at 0.570 V (vs Ag/AgCl) at the noted experimental conditions.

Preparation of *trans*-Ru_2(DMBA)$_4$(H-*gem*-DEE)$_2$ (1). $Ru_2(DMBA)_4(NO_3)_2$ (0.092 g, 0.101 mmol) was dissolved in THF (20 mL), to which were added **L1** (0.023 g, 0.220 mmol) and Et_3N (1 mL). Upon the addition of Et_3N, the reaction mixture turned from green to wine red in ca. 3 min and was stirred for an additional 3 h. TLC analysis (1:3 EtOAc/hexanes) revealed a red product (**1**) and a reddish-brown species just above the baseline. After removal of the solvent, the resulting red residue was purified via column chromatography (1:6 → 1:1 EtOAc/hexanes) followed by recrystallization from THF/MeOH (1:3, v/v) to yield **1** as a red crystalline solid. Yield: 0.020 g (0.020 mmol, 20% based on Ru). Data for **1**. R_f = 0.72 (1:3 EtOAc/hexanes). ^{1}H NMR ($CDCl_3$, δ): 7.41−7.38 (12H, Ph*H*), 6.98−6.95 (8H, Ph*H*), 3.23 (24H, N*Me*), 2.86 (2H, C_2H), 2.10 (12H, *Me* (*gem*-DEE)). nESI-MS (*m*/*e*, based on ^{101}Ru): 998, corresponding to $[M + H]^+$. HR-nESI-MS (*m*/*e*, based on ^{101}Ru): 997.826, corresponding to $[M + H]^+$ ($C_{52}H_{58}N_8Ru_2$, calcd 997.834). Vis−NIR [λ_{max}, nm (ε, M^{-1} cm^{-1})]: 890 (2210), 506 (14 600). FT-IR (neat, ν, cm^{-1}): 2076 (−C≡C−H), 2057 (Ru−C≡C−). CV [$E_{1/2}$/V, ΔE_p/V, $i_{backward}/i_{forward}$]: **B**, 0.502, 0.034, 0.903; **C**, −1.154, 0.036, 0.935; E_{pc} (**D**), −1.514.

dx.doi.org/10.1021/ic202720c | *Inorg. Chem.* 2012, 51, 3261−3269

Preparation of *trans*-$Ru_2(DMBA)_4(^iPr_3Si$-*gem*-DEE)$_2$ (2). $Ru_2(DMBA)_4(NO_3)_2$ (0.151 g, 0.165 mmol) was dissolved in THF (30 mL), to which were added **L2** (0.094 g, 0.363 mmol) and Et_2NH (1 mL). Upon the addition of Et_2NH, the reaction mixture turned from green to wine red in ca. 3 min and was stirred for an additional 3 h. TLC analysis (1:3 EtOAc/hexanes) revealed compound **2** as the sole product formed. The reaction mixture was then filtered through a 2 cm silica gel plug to remove any residual $Ru_2(DMBA)_4(NO_3)_2$. After removal of the solvent, the resulting red residue was purified via recrystallization from THF/MeOH (1:4, v/v) to yield a red crystalline solid. Yield: 0.166 g (0.127 mmol, 77% based on Ru). Data for **2**. R_f = 0.83 (1:3 EtOAc/hexanes). ^{1}H NMR ($CDCl_3$, δ): 7.39−7.36 (12H, Ph*H*), 6.96−6.94 (8H, Ph*H*), 3.22 (24H, N*Me*), 2.12 (12H, *Me* (*gem*-DEE), 0.95 (21H, $^iPr_3$Si). nESI-MS (*m*/*e*, based on ^{101}Ru): 1310, corresponding to $[M + H]^+$. HR-nESI-MS (*m*/*e*, based on ^{101}Ru): 1309.620, corresponding to $[M + H]^+$ ($C_{70}H_{98}N_8Si_2Ru_2$, calcd 1309.613). Vis−NIR [λ_{max}, nm (ε, M^{-1} cm^{-1})]: 890 (2330), 507 (14 600). FT-IR (neat, ν, cm^{-1}): 2140 (−C≡C−Si^{i}Pr$_3$), 2065 (Ru−C≡C−). CV [$E_{1/2}$/V, ΔE_p/V, $i_{backward}/i_{forward}$]: **B**, 0.496, 0.034, 0.905; **C**, −1.159, 0.037, 0.931; E_{pc}(**D**), −1.496.

Preparation of *trans*-$Ru_2(DMBA)_4$(Fc-*gem*-DEE)$_2$ (3). $Ru_2(DMBA)_4(NO_3)_2$ (0.230 g, 0.251 mmol) was dissolved THF (40 mL), to which were added 2.2 equiv of **L3** (0.160 g, 0.552 mmol) of **L3** and 5 mL of Et_2NH. Upon the addition of Et_2NH, the reaction mixture began to turn from green to red in ca. 15 min. The reaction was stirred for an additional 3 h. TLC analysis (1:3 EtOAc/hexanes) revealed the formation of **3** along with unreacted ligand (**L3**) and $Ru_2(DMBA)_4(NO_3)_2$. Removal of the solvent yielded a red residue, which was redissolved in EtOAc/hexanes (1:6, v/v) and filtered through a 3 cm silica gel plug to remove the residual **L3** ligand and $Ru_2(DMBA)_4(NO_3)_2$. After removal of the solvent, the resulting red residue was further purified via recrystallization from THF/hexanes (1:9, v/v) to yield a red crystalline solid. Yield: 0.164 g (0.120 mmol, 48% based on Ru). Data for **3**. R_f = 0.66 (1:3 EtOAc/hexanes). ^{1}H NMR ($CDCl_3$, δ): 7.37−7.35 (12H, Ph*H*), 6.99−6.96 (8H, Ph*H*), 4.25 (4H, Cp*H*), 4.04 (14H, Cp*H*), 3.29 (24H, N*Me*), 2.12 (12H, *Me* (*gem*-DEE). nESI-MS (*m*/*e*, based on ^{101}Ru): 1366, corresponding to $[M + H]^+$. HR-nESI-MS (*m*/*e*, based on ^{101}Ru): 1366.285, corresponding to $[M + H]^+$ ($C_{72}H_{74}N_8Fe_2Ru_2$, calcd 1366.275). Vis−NIR [λ_{max}, nm (ε, M^{-1} cm^{-1})]: 890 (2290), 504 (15 400). FT-IR (neat, ν, cm^{-1}): 2140 (−C≡C−Fc)), 2070 (Ru−C≡C−). CV [$E_{1/2}$/V, ΔE_p/V, $i_{backward}/i_{forward}$]: **Fc**, 0.690, 0.035, 0.100; **A**, 0.467, 0.033, 0.500; **B**, −1.156, 0.033, 0.870; E_{pc}(**C**), −1.552.

Preparation of *trans*-$Ru_2(DMBA)_4$(NP-*gem*-DEE)$_2$ (4). $Ru_2(DMBA)_4(NO_3)_2$ (0.101 g, 0.110 mmol) was dissolved in THF (35 mL), to which were added **L4** (0.054 g, 0.242 mmol) and 2 mL of Et_2NH. Upon the addition of Et_2NH, the reaction mixture turned from green to red in ca. 6 min and the reaction was stirred for an additional 3 h. TLC analysis (1:3 EtOAc/hexanes) revealed compound **4** as the sole product formed. The reaction mixture was then filtered through a 2 cm silica gel plug to remove any residual $Ru_2(DMBA)_4(NO_3)_2$. After removal of the solvent, the resulting red residue was purified via recrystallization from 1:9 THF/hexanes to yield a red crystalline solid. Yield: 0.094 g (0.076 mmol, 68% based on Ru). Data for **4**. R_f = 0.58 (1:3 EtOAc/hexanes). ^{1}H NMR ($CDCl_3$, δ): 8.18−8.15 (4H, O_2NPh*H*), 7.58−7.55 (4H, Ph*H*), 7.42−7.39 (12H, Ph*H*), 6.98−6.96 (8H, Ph*H*), 3.26 (24H, N*Me*), 2.17 (12H, *Me* (*gem*-DEE). nESI-MS (*m*/*e*, based on ^{101}Ru): 1240, corresponding to $[M + H]^+$. HR-nESI-MS (*m*/*e*, based on ^{101}Ru): 1240.436, corresponding to $[M + H]^+$ ($C_{64}H_{64}N_{10}O_4Ru_2$, calcd 1240.425). Vis−NIR [λ_{max}, nm (ε, M^{-1} cm^{-1})]: 865 (1960), 497 (14 900). FT-IR (neat, ν, cm^{-1}): 2195 (−C≡C−NP), 2065 (Ru−C≡C−). CV [$E_{1/2}$/V, ΔE_p/V, $i_{backward}/i_{forward}$]: **A**, 0.485, 0.041, 0.870.

Preparation of *trans*-$Ru_2(DMBA)_4$(DMAP-*gem*-DEE)$_2$ (5). *Method A.* $Ru_2(DMBA)_4(NO_3)_2$ (0.106 g, 0.116 mmol) was dissolved in THF [or 2:1 (v/v) THF/MeOH], to which were added **L5** (or TMS-**L5**) (2.2 equiv, 0.255 mmol) and 5 mL of Et_2NH (or excess K_2CO_3). Upon the addition of a base, the reaction mixture began to turn from green to red in ca. 30 min. The reaction was stirred for an additional 3 h. Ensuing TLC analysis (1:1:3 CH_2Cl_2/Et_3N/hexanes) revealed the formation of **5** along with a brown-red product (R_f = 0.45) and unreacted starting materials. The reaction mixture was then filtered through a plug of Celite to remove the residual $Ru_2(DMBA)_4(NO_3)_2$. After removal of the solvent, the resulting red residue was purified via recrystallization from THF/hexanes (1:15, v/v) to yield a red crystalline solid. Yield: 0.038 g (0.031 mmol, 27% based on Ru).

Method B. **L5** (0.116 g, 0.520 mmol) was lithiated with *n*-BuLi (1.1 equiv of **L5**) in a THF solution to form Li-**L5** *in situ*. Li-**L5** was then transferred via a cannula to a THF solution of $Ru_2(DMBA)_4Cl_2$ (0.207 g, 0.240 mmol). Following transfer, the reaction mixture changed immediately from brown to deep red-purple. The reaction was stirred overnight to ensure complete reaction. Ensuing TLC analysis (1:1:3 CH_2Cl_2/Et_3N/hexanes) revealed compound **5** as the sole product. The solvent was then removed, and the resulting red-purple residue was redissolved in CH_2Cl_2/hexanes (1:3, v/v) and filtered quickly through a plug of Celite. After removal of the solvent, the resulting red residue was recrystallized from EtOAc/hexanes (1:5, v/v) to yield a red-purple crystalline solid. Yield: 0.220 g (0.180 mmol, 74% based on Ru).

Data for **5**. R_f = 0.64 (1:1:3 CH_2Cl_2/Et_3N/hexanes). ^{1}H NMR ($CDCl_3$, δ): 7.39−7.37 (16H, Ph*H*), 6.98−6.95 (8H, Ph*H*), 6.53−6.51 (4H, Ph*H*), 3.26 (24H, N*Me*), 2.90 (12H, PhN*Me*), 2.24 (12H, *Me* (*gem*-DEE). nESI-MS (*m*/*e*, based on ^{101}Ru): 1236, corresponding to $[M + H]^+$. HR-nESI-MS (*m*/*e*, based on ^{101}Ru): 1236.557, corresponding to $[M + H]^+$ ($C_{68}H_{76}N_{10}Ru_2$, calcd 1236.566). Vis−NIR [λ_{max}, nm (ε, M^{-1} cm^{-1})]: 890 (2460), 505 (15 400). FT-IR (neat, ν, cm^{-1}): 2193 (−C≡C−DMAP), 2071 (Ru−C≡C−). CV [$E_{1/2}$/V, ΔE_p/V, $i_{backward}/i_{forward}$]: **A**, 0.434, 0.041, 0.780; **B**, −1.165, 0.038, 0.360; **C**, −1.541, 0.049, 1.000; E_{pa}(-**NMe$_2$**), 0.944.

Preparation of *trans*-$Ru_2(DMBA)_4(C{\equiv}CSi^iPr_3)_2$ (6). $Ru_2(DMBA)_4(NO_3)_2$ (0.180 g, 0.197 mmol) was dissolved in THF (30 mL), to which was added HC≡CSi^{i}Pr$_3$ (0.097 mL, 0.432 mmol) and Et_3N (2 mL). Upon the addition of Et_3N, the reaction mixture turned from green to wine red in ca. 2 min and was stirred for an additional 3 h to yield **6** as the sole product. The reaction mixture was then filtered through a 2 cm silica gel plug to remove any residual $Ru_2(DMBA)_4(NO_3)_2$. After removal of the solvent, the resulting red residue was purified via recrystallization from THF/MeOH (1:3, v/v) to yield a red crystalline solid. Yield: 0.191 g (0.166 mmol, 84% based on Ru). Data for **6**. R_f = 0.85 (1:3 EtOAc/hexanes). ^{1}H NMR ($CDCl_3$, δ): 7.45−7.43 (12H, Ph*H*), 7.00−6.97 (8H, Ph*H*), 3.28 (24H, N*Me*), 0.97 (21H, $^iPr_3$Si). nESI-MS (*m*/*e*, based on ^{101}Ru): 1155, corresponding to $[M + H]^+$. FT-IR (neat, ν, cm^{-1}): 1996 (Ru−C≡C−Si^{i}Pr$_3$). CV [$E_{1/2}$/V, ΔE_p/V, $i_{backward}/i_{forward}$]: **A**, 0.585, 0.041, 0.858; **B**, −1.138, 0.038, 1.000.

X-ray Data Collection, Processing, and Structure Analysis and Refinement for Crystals **2** *and* **3**. Single crystals of compounds **2** and **3** were grown via the slow cooling of a THF/MeOH solution (1:3, v/v) and the slow evaporation of a THF/benzene/hexanes solution (1:1:9, v/v/v), respectively. X-ray diffraction data were collected on a Rigaku RAPID-II image plate diffractometer using Cu Kα radiation (λ = 1.541 84 Å) at 150 K, and the structures were solved using the structure solution program *DIRDIF2008*[39] and refined using *SHELX-TL*.[40] Relevant information on the data collection and figures of merit of the final refinement is listed in Table 3.

Computational Methods. Ground-state geometries of model compounds **2′**, **7**, **4′**, and **5′** were fully optimized using the DFT method B3LYP (Becke's three-parameter hybrid functional using the Lee−Yang−Parr correlation functional).[41] The geometry of model compound **2′** was fully optimized from the crystal structure of **2**, while those of **7**, **4′**, and **5′** were assembled based on the truncated crystal structure of **2**. Both Si^{i}Pr$_3$ ligands in **2** were replaced by $-C_6H_5$ (**7**), 4-$C_6H_4NO_2$ (**4′**), or 4-$C_6H_4NMe_2$ (**5′**), followed by full optimization. In the calculations, quasi-relativistic pseudopotentials of the 16 ruthenium valence electrons were employed and the LanL2DZ basis sets associated with the pseudopotential were adopted. All of the calculations were performed using the *Gaussian03* program package.[36] No negative frequency was observed in the vibrational frequency analysis, which

dx.doi.org/10.1021/ic202720c | *Inorg. Chem.* 2012, 51, 3261−3269

Table 3. Crystal Data for Compounds 2 and 3

	2·THF	3
molecular formula	$C_{74}H_{106}N_8ORu_2Si_2$	$C_{72}H_{74}Fe_2N_8Ru_2Si_2$
fw	1382.03	1365.28
space group	$P\bar{1}$	$C2/c$(No. 15)
a, Å	10.626(2)	25.4583(9)
b, Å	16.654(3)	20.7805(7)
c, Å	21.360(3)	13.8410(4)
α, deg	80.51(8)	
β, deg	79.91(10)	120.020(2)
γ, deg	87.79(12)	
V, Å^3	3671(1)	6340.1(4)
Z	2	4
ρ_{calcd}, g cm^{-3}	1.250	1.430
μ, mm^{-1}	4.071	7.754
T, K	150	150
no. of rflns collected	58683	34760
no. of indep rflns	9274 [R(int) = 0.097]	5977 [R(int) = 0.048]
final R indices [$I > 2\sigma(I)$]	R1 = 0.078, wR2 = 0.218	R1 = 0.037, wR2 = 0.096

indicates that these *gem*-DEE-substituted diruthenium complexes are metastable equilibrium structures.

■ ASSOCIATED CONTENT

Supporting Information

Vis−NIR spectra for **1**, **3**, and **6**, equilibrium structures and optimized bond lengths and angles from DFT calculations for model compounds **2′**, **4′**, **5′**, and **7**, nESI-MS spectra for **2** and **6**, and X-ray crystallographic files in CIF format for the structure determination of compounds **2** and **3**. This material is available free of charge via the Internet at http://pubs.acs.org.

■ AUTHOR INFORMATION

Corresponding Author

*E-mail: tren@purdue.edu.

Notes

The authors declare no competing financial interest.

■ ACKNOWLEDGMENTS

We gratefully acknowledge financial support from the National Science Foundation (Grant CHE 1057621) and Purdue University.

■ REFERENCES

(1) Bosshard, C.; Sutter, K.; Pretre, P.; Hulliger, J.; Florsheimer, M.; Kaatz, P.; Gunter, P. *Organic Nonlinear Optical Materials*; Gordon and Breach: Amsterdam, The Netherlands, 1995. Gubler, U.; Bosshard, C. *Adv. Polym. Sci.* **2002**, *158*, 123. Klokkenburg, M.; Lutz, M.; Spek, A. L.; van der Maas, J. H.; van Walree, C. A. *Chem.—Eur. J.* **2003**, *9*, 3544. Prasad, P. N.; Williams, D. J. *Introduction to Nonlinear Optical Effects in Molecules and Polymers*; Wiley: New York, 1991. van Walree, C. A.; Kaats-Richters, V. E. M.; Veen, S. J.; Wieczorek, B.; van der Wiel, J. H.; van der Wiel, B. C. *Eur. J. Org. Chem.* **2004**, *2004*, 3046. Zhao, Y.; Slepkov, A. D.; Akoto, C. O.; McDonald, R.; Hegmann, F. A.; Tykwinski, R. R. *Chem.—Eur. J.* **2005**, *11*, 321. Skotheim, T. A., Elsenbaumer, R. L., Reynolds, J. R., Eds. *Handbook of Conducting Polymers*; Marcel Dekker: New York, 1998. Mullen, K., Wegner, G., Eds. *Electronic Materials: The Oligomer Approach*; VCH: Weinheim, Germany, 1997. Martin, R. E.; Diederich, F. *Angew. Chem., Int. Ed.* **1999**, *38*, 1350. Zhou, G.-J.; Wong, W.-Y. *Chem. Soc. Rev.* **2011**, *40*, 2541.

(2) Miller, R. D.; Michl, J. *Chem. Rev.* **1989**, *89*, 1359.

(3) Bakkers, E. P. A. M.; Marsman, A. W.; Jenneskens, L. W.; Vanmaekelbergh, D. L. *Angew. Chem., Int. Ed.* **2000**, *39*, 2297. Hoogesteger, F. J.; van Walree, C. A.; Jenneskens, L. W.; Roest, M. R.; Verhoeven, J. W.; Schuddeboom, W.; Piet, J. J.; Warman, J. M. *Chem.—Eur. J.* **2000**, *6*, 2948.

(4) van Walree, C. A.; Kooijman, H.; Spek, A. L.; Zwikker, J. W.; Jenneskens, L. W. *J. Chem. Soc., Chem. Commun.* **1995**, 35. van Walree, C. A.; Roest, M. R.; Schuddeboom, W.; Jenneskens, L. W.; Verhoeven, J. W.; Warman, J. M.; Kooijman, H.; Spek, A. L. *J. Am. Chem. Soc.* **1996**, *118*, 8395.

(5) Phelan, N. F.; Orchin, M. *J. Chem. Educ.* **1968**, *45*, 633.

(6) Nielsen, M. B.; Diederich, F. *Chem. Rev.* **2005**, *105*, 1837.

(7) Tykwinski, R. R.; Zhao, Y. M. *Synlett* **2002**, 1939. Gholami, M.; Tykwinski, R. R. *Chem. Rev.* **2006**, *106*, 4997.

(8) Hopf, H. *Classics in Hydrocarbon Chemistry*; Wiley-VCH: Weinheim, Germany, 2000.

(9) Zhao, Y.; Tykwinski, R. R. *J. Am. Chem. Soc.* **1999**, *121*, 458.

(10) Zhao, Y. M.; Campbell, K.; Tykwinski, R. R. *J. Org. Chem.* **2002**, *67*, 336.

(11) Burri, E.; Diederich, F.; Brandsted-Nielsen, M. *Helv. Chim. Acta* **2002**, *85*, 2169. Zhao, Y.; McDonald, R.; Tykwinski, R. R. *Chem. Commun.* **2000**, 77.

(12) Zhao, Y.; McDonald, R.; Tykwinski, R. R. *J. Org. Chem.* **2002**, *67*, 2805.

(13) Bruschi, M.; Giuffreda, M. G.; Luthi, H. P. *Chem.—Eur. J.* **2002**, *8*, 4216.

(14) Solomon, G. C.; Andrews, D. Q.; Goldsmith, R. H.; Hansen, T.; Wasielewski, M. R.; Van Duyne, R. P.; Ratner, M. A. *J. Am. Chem. Soc.* **2008**, *130*, 17301.

(15) Hagihara, N.; Sonogashira, K.; Takahashi, S. *Adv. Polym. Sci.* **1980**, *40*, 149. Nast, R. *Coord. Chem. Rev.* **1982**, *47*, 89. Paul, F.; Lapinte, C. *Coord. Chem. Rev.* **1998**, *178−180*, 431. Wong, W.-Y.; Ho, C.-L. *Coord. Chem. Rev.* **2006**, *250*, 2627.

(16) Szafert, S.; Gladysz, J. A. *Chem. Rev.* **2006**, *106*, 1.

(17) Lenarvor, N.; Toupet, L.; Lapinte, C. *J. Am. Chem. Soc.* **1995**, *117*, 7129. Hamon, P.; Justaud, F.; Cador, O.; Hapiot, P.; Rigaut, S.; Toupet, L.; Ouahab, L.; Stueger, H.; Hamon, J.-R.; Lapinte, C. *J. Am. Chem. Soc.* **2008**, *130*, 17372.

(18) Brady, M.; Weng, W.; Zou, Y.; Seyler, J. W.; Amoroso, A. J.; Arif, A. M.; Bohme, M.; Frenking, G.; Gladysz, J. A. *J. Am. Chem. Soc.* **1997**, *119*, 775.

(19) Bruce, M. I.; Low, P. J.; Costuas, K.; Halet, J.-F.; Best, S. P.; Heath, G. A. *J. Am. Chem. Soc.* **2000**, *122*, 1949. Fox, M. A.; Roberts, R. L.; Baines, T. E.; Guennic, B. L.; Halet, J.-F.; Hartl, F.; Yufit, D. S.; Albesa-Jové, D.; Howard, J. A. K.; Low, P. J. *J. Am. Chem. Soc.* **2008**, *130*, 3566. Olivier, C.; Costuas, K.; Choua, S.; Maurel, V.; Turek, P.; Saillard, J.-Y.; Touchard, D.; Rigaut, S. *J. Am. Chem. Soc.* **2010**, *132*, 5638. Liu, S. H.; Chen, Y.; Wan, K. L.; Wen, T. B.; Zhou, Z.; Lo, M. F.; Williams, I. D.; Jia, G. *Organometallics* **2002**, *21*, 4984. Li, F.; Cheng, J.; Chai, X.; Jin, S.; Wu, X.; Yu, G.-A.; Liu, S. H.; Chen, G. Z. *Organometallics* **2011**, *30*, 1830. Ren, T.; Zou, G.; Alvarez, J. C. *Chem. Commun.* **2000**, 1197. Xu, G.-L.; Zou, G.; Ni, Y.-H.; DeRosa, M. C.; Crutchley, R. J.; Ren, T. *J. Am. Chem. Soc.* **2003**, *125*, 10057. Xi, B.; Liu, I. P. C; Xu, G.-L.; Choudhuri, M. M. R.; DeRosa, M. C.; Crutchley, R. J.; Ren, T. *J. Am. Chem. Soc.* **2011**, *133*, 15094.

(20) Campbell, K.; Johnson, C. A.; McDonald, R.; Ferguson, M. J.; Haley, M. M.; Tykwinski, R. R. *Angew. Chem., Int. Ed.* **2004**, *43*, 5967. Campbell, K.; McDonald, R.; Ferguson, M. J.; Tykwinski, R. R. *J. Organomet. Chem.* **2003**, *683*, 379. Campbell, K.; McDonald, R.; Ferguson, M. J.; Tykwinski, R. R. *Organometallics* **2003**, *22*, 1353.

(21) Diederich, F.; Faust, R.; Gramlich, V.; Seiler, P. *Chem. Commun.* **1994**, 2045. Faust, R.; Diederich, F.; Gramlich, V.; Seiler, P. *Chem.—Eur. J.* **1995**, *1*, 111.

(22) Lu, W.; Zhu, N.; Che, C.-M. *J. Organomet. Chem.* **2003**, *670*, 11.

(23) Akita, M.; Tanaka, Y.; Naitoh, C.; Ozawa, T.; Hayashi, N.; Takeshita, M.; Inagaki, A.; Chung, M.-C. *Organometallics* **2006**, *25*, 5261.

(24) Bruce, M. I.; Zaitseva, N. N.; Low, P. J.; Skelton, B. W.; White, A. H. *J. Organomet. Chem.* **2006**, *691*, 4273.

(25) Forrest, W. P.; Cao, Z.; Fanwick, P. E.; Hassell, K. M.; Ren, T. *Organometallics* **2011**, *30*, 2075.
(26) Xu, G.-L.; Jablonski, C. G.; Ren, T. *Inorg. Chim. Acta* **2003**, *343*, 387.
(27) Xu, G.-L.; Jablonski, C. G.; Ren, T. *J. Organomet. Chem.* **2003**, *683*, 388. Ying, J.-W.; Cordova, A.; Ren, T. Y.; Xu, G.-L.; Ren, T. *Chem.—Eur. J.* **2007**, *13*, 6874.
(28) Hurst, S. K.; Xu, G.-L.; Ren, T. *Organometallics* **2003**, *22*, 4118.
(29) Ren, T. *Organometallics* **2005**, *24*, 4854.
(30) Lin, C.; Ren, T.; Valente, E. J.; Zubkowski, J. D. *J. Chem. Soc., Dalton Trans.* **1998**, 571.
(31) Liu, I. P.-C.; Ren, T. *Inorg. Chem.* **2009**, *48*, 5608.
(32) Zhao, Y. M.; Zhou, N. Z.; Slepkov, A. D.; Ciulei, S. C.; McDonald, R.; Hegmann, F. A.; Tykwinski, R. R. *Helv. Chim. Acta* **2007**, *90*, 909.
(33) Xu, G.-L.; Campana, C.; Ren, T. *Inorg. Chem.* **2002**, *41*, 3521.
(34) Xu, G.-L.; DeRosa, M. C.; Crutchley, R. J.; Ren, T. *J. Am. Chem. Soc.* **2004**, *126*, 3728. Xi, B.; Xu, G.-L.; Fanwick, P. E.; Ren, T. *Organometallics* **2009**, *28*, 2338.
(35) Xu, G.-L.; Crutchley, R. J.; DeRosa, M. C.; Pan, Q.-J.; Zhang, H.-X.; Wang, X.; Ren, T. *J. Am. Chem. Soc.* **2005**, *127*, 13354.
(36) Frisch, M. J.; Trucks, G. W.; Schlegel, H. B.; Scuseria, G. E.; Robb, M. A.; Cheeseman, J. R.; Montgomery, J. A., Jr.; Vreven, T.; Kudin, K. N.; Burant, J. C.; Millam, J. M.; Iyengar, S. S.; Tomasi, J.; Barone, V.; Mennucci, B.; Cossi, M.; Scalmani, G.; Rega, N.; Petersson, G. A.; Nakatsuji, H.; Hada, M.; Ehara, M.; Toyota, K.; Fukuda, R.; Hasegawa, J.; Ishida, M.; Nakajima, T.; Honda, Y.; Kitao, O.; Nakai, H.; Klene, M.; Li, X.; Knox, J. E.; Hratchian, H. P.; Cross, J. B.; Bakken, V.; Adamo, C.; Jaramillo, J.; Gomperts, R.; Stratmann, R. E.; Yazyev, O.; Austin, A. J.; Cammi, R.; Pomelli, C.; Ochterski, J. W.; Ayala, P. Y.; Morokuma, K.; Voth, G. A.; Salvador, P.; Dannenberg, J. J.; Zakrzewski, V. G.; Dapprich, S.; Daniels, A. D.; Strain, M. C.; Farkas, O.; Malick, D. K.; Rabuck, A. D.; Raghavachari, K.; Foresman, J. B.; Ortiz, J. V.; Cui, Q.; Baboul, A. G.; Clifford, S.; Cioslowski, J.; Stefanov, B. B.; Liu, G.; Liashenko, A.; Piskorz, P.; Komaromi, I.; Martin, R. L.; Fox, D. J.; Keith, T.; Al-Laham, M. A.; Peng, C. Y.; Nanayakkara, A.; Challacombe, M.; Gill, P. M. W.; Johnson, B.; Chen, W.; Wong, M. W.; Gonzalez, C.; Pople, J. A. *Gaussian03*, revision D.02; Gaussian, Inc.: Wallingford, CT, 2003.
(37) Cao, Z.; Ren, T. *Organometallics* **2011**, *30*, 245.
(38) Zhao, Y.; Zhou, N.; Slepkov, A. D.; Ciulei, S. C.; McDonald, R.; Hegmann, F. A.; Tykwinski, R. R. *Helv. Chim. Acta* **2007**, *90*, 909.
(39) Beurskens, P. T.; Beurskens, G.; deGelder, R.; Garcia-Granda, S.; Gould, R. O.; Smits, J. M. M. *The DIRDIF2008 Program System*; Crystallography Laboratory, University of Nijmegen: Nijmegen, The Netherlands, 2008.
(40) Sheldrick, G. M. *Acta Crystallogr., Sect. A* **2008**, *64*, 112.
(41) Becke, A. D. *J. Chem. Phys.* **1993**, *98*, 5648. Stephens, P. J.; Devlin, F. J.; Chabalowski, C. F.; Frisch, M. J. *J. Phys. Chem.* **1994**, *98*, 11623.